Difficult Job

- Abell 2319 Optical Sky Survey
- Despite the high degree of difficulty Abell did a fantastic job- but catalog suffers from incompleteness and projection effects

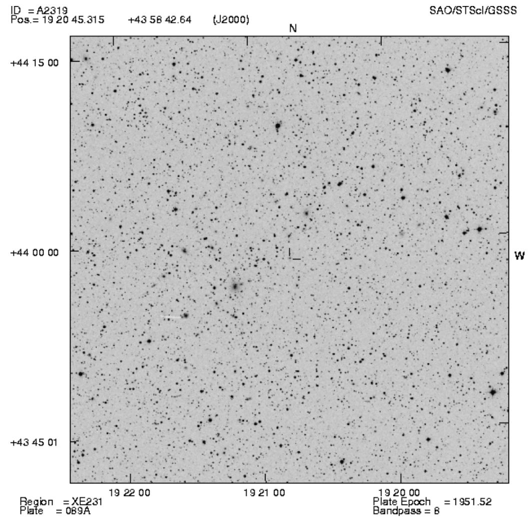

X-ray image

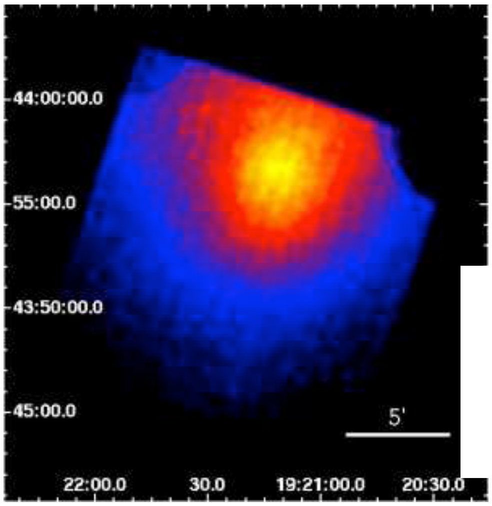

Table 1. Table 1: Abell Richness Class

	Abell 0	Abell 1	Abell 2	Abell 3
N_{Abell}	35–45	45–75	75–125	125–200
Number	~ 1000	1224	383	6
σ (km s^{-1})	600	750	950	1250
Mass (10^{14}M$_{\odot}$)	2	4	9	15

26

- FR I radio galaxies (low power radio galaxies, which possess an "edge-darkened" radio morphology) occur more frequently in clusters than in the field because their hosts are always luminous ellipticals
- Similar 'tailed' radio galaxies(a subset of FRIs) 'only' occur in clusters (Giacintucci et al 2009) Fomalont & Bridle 1978; Burns & Owen 1979; more recently Blanton et al. 2000, 2001 and 2003; Smolcic et al. 2007;

2 Giacintucci & Venturi: Tailed radio galaxies as tracers of galaxy clusters

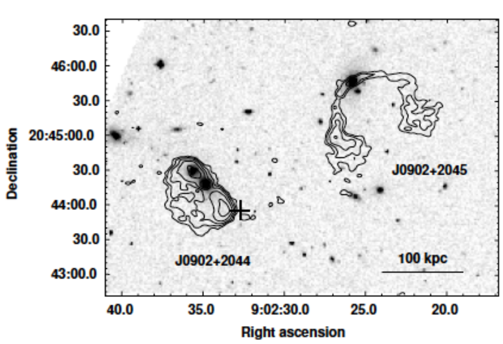

Fig. 1. GMRT 610 MHz contours of the two tailed radio galaxies discovered at ~27 ′ from the galaxy cluster Z2089. The image is corrected for the primary beam. The radio contours are overlaid on the red optical image from the SDSS. The resolution of the radio image is 6.5″ × 4.5″, p.a. 80°. The lowest contour is 0.5 mJy b^{-1}, and each contour increases by a factor of two. The cross indicates the centre of the candidate galaxy cluster NSC J090232+204358. The linear scale is 1″=1.56 kpc (see Sect. 3)

Radio Selection

Galaxies around high z FRI candidat

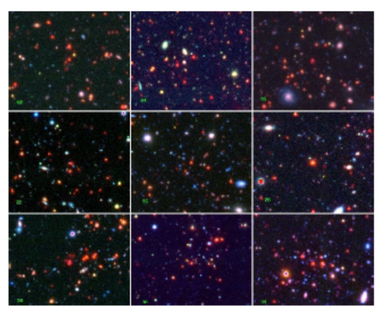

***Figure** 2 RGB images of nine cluster candidates found around our high-z FR I candidates. The "color" images are obtained using Spitzer data at 3.6μm for the R channel, z-band for the G channel, and V-band for the B channel. The projected scale of each image is ~110" x 90". The photometric redshifts of the candidates are between 1.30 and 2.04.*

These radio techniques enable clusters to be found, but there is no relation
Between radio properties and other properties of the cluster

27

Cluster Formation

- Cluster mergers are thought to be the prime mechanism of massive cluster formation in a hierarchical universe (White and Frenk 1991)
- the most energetic events in the universe since the big bang. These mergers with infall velocities of ~2000 km/s and total masses of $10^{15}\,M_\odot$ have a kinetic energy of 10^{65} ergs.
- The shocks and structures generated in the merger have a important influence on cluster shape, luminosity and evolution and may generate large fluxes of relativistic particles

Numerical Simulation of a Merger

- X-ray contours with kT in color, dark matter distribution, velocity vectors and how the two gas components mix (0.3 and 3.5Gyr after closest approach)

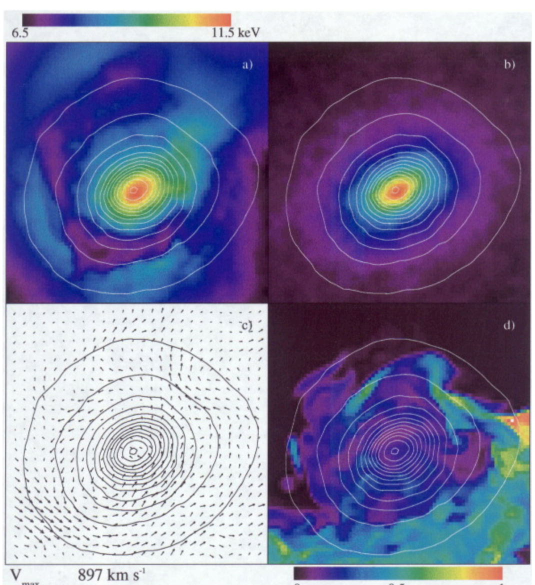

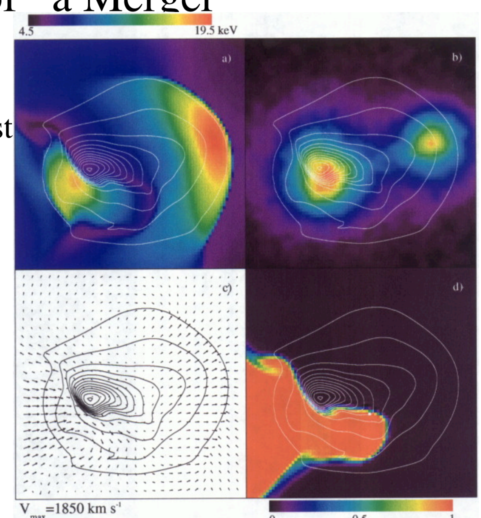

•Roettiger, Stone and Mushotzky 1998 first detailed simulations of a merger- trying to match A754

X-ray Images of Mergers

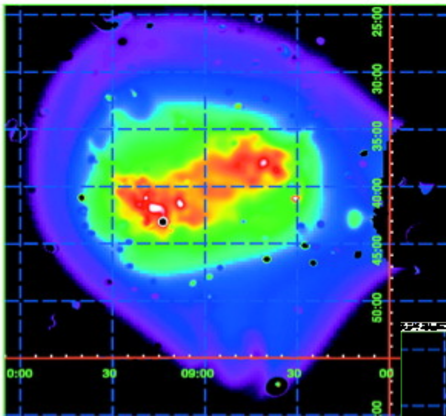

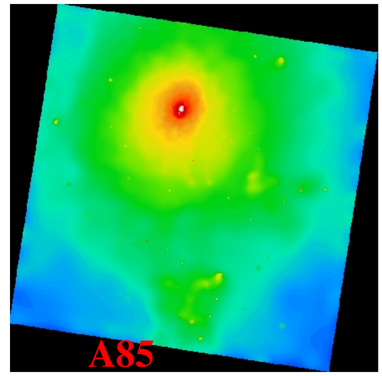

- A754 (Henry et al 2004) pressure and x-ray intensity images

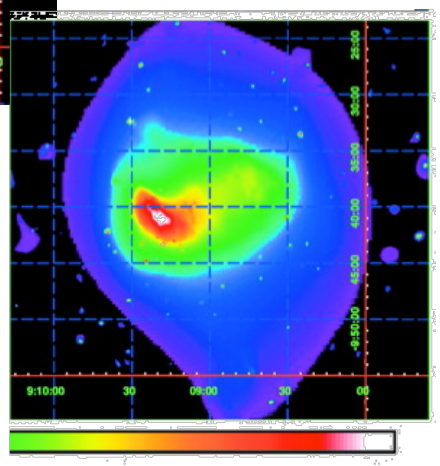

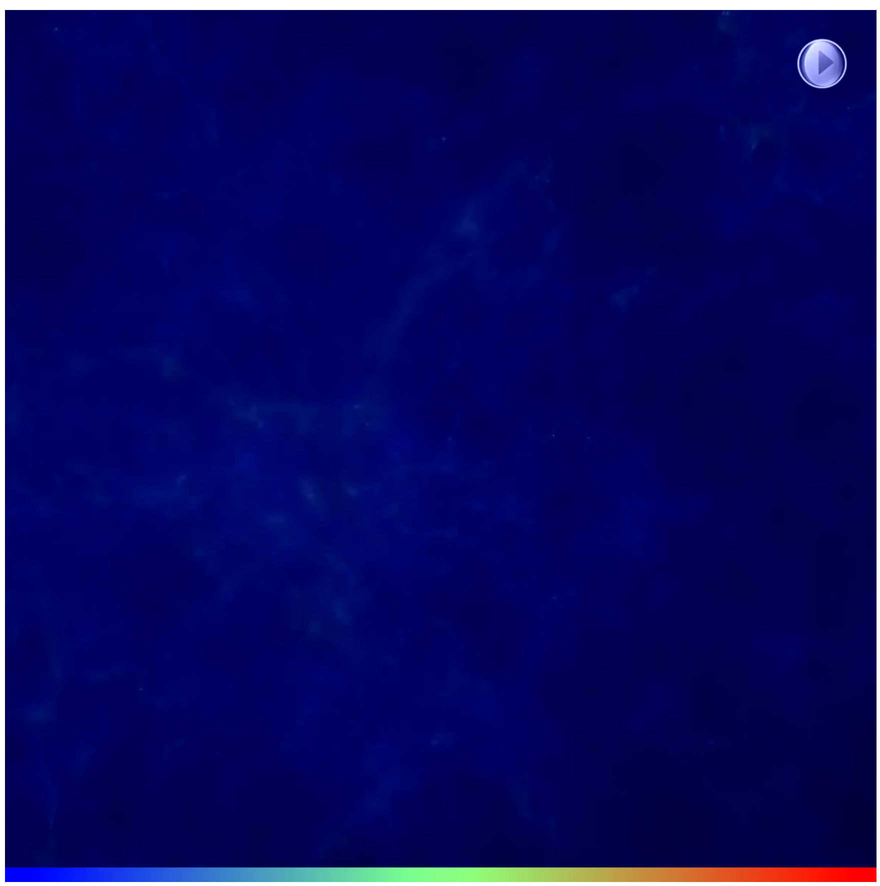

- Movie from http://www.multidark.org/MultiDark/pages/ImagesMovies.jsp

- made by G. Yepes

What is a Merger Tree

- In LCDM cosmology structure grows by the merging of bound systems + infall
- The fraction of contribution of each component depends on time and mass.

n

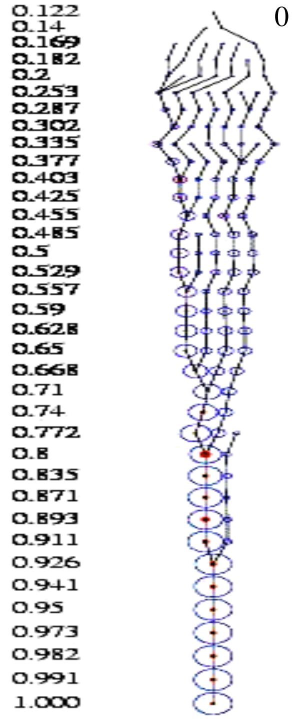

R. Wechsler

Brightest Cluster Galaxies

- most luminous and most massive galaxies in the Universe at the present epoch.
- At low redshift, these objects exhibit a small dispersion in their aperture luminosities
- lie close to the peaks of the X–ray emission
- Have small relative velocity to cluster average
- Different luminosity profiles than typical cluster elliptical galaxies- show a shallow very large 'envelope'
- Very large number of globular clusters

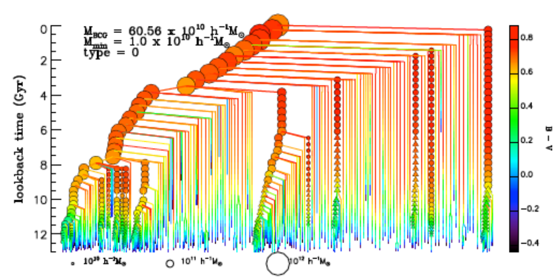

Figure 1. BCG merger tree. Symbols are colour–coded as a function of B - V colour and their area scales with the stellar mass. Only progenitors more massive than 10^{10} $M_\odot$ h^{-1} are shown with symbols. Circles are used for galaxies that reside in the FOF group inhabited by the main branch. Triangles show galaxies that have not yet joined this FOF group.

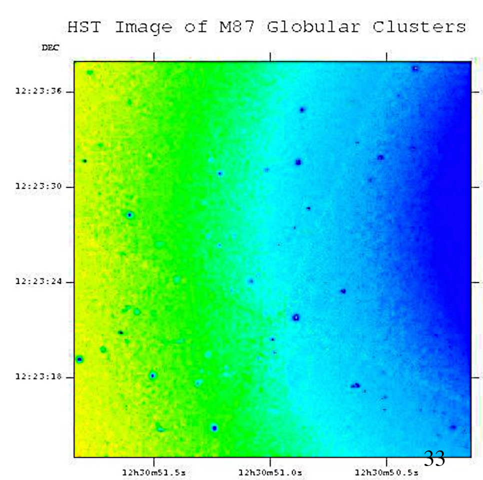

Cosmology

- The rate of cluster growth is a strong function of cosmological parameters

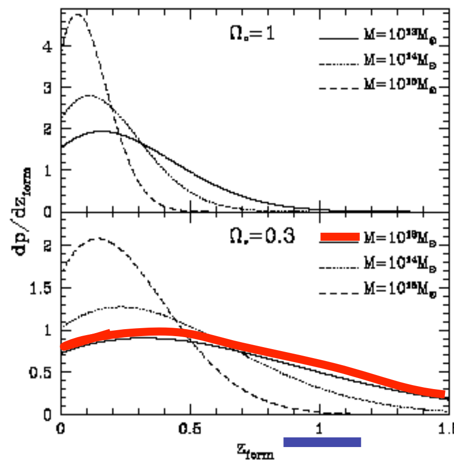

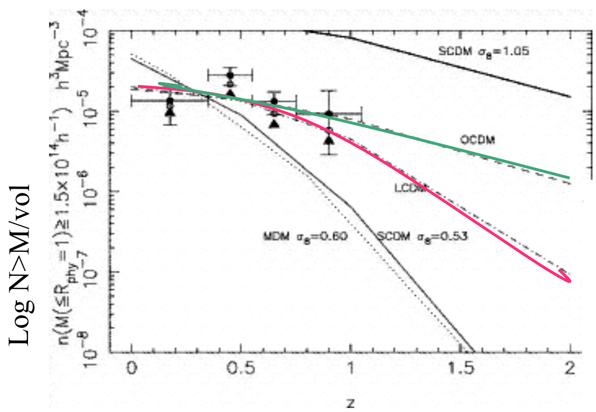

Bahcall,Cen,Fan

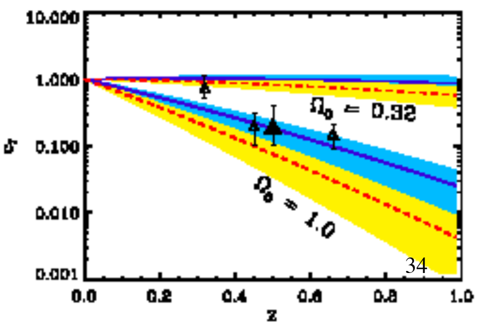

Mass Function

- The number of clusters per unit mass (optical luminosity, x-ray luminosity, velocity dispersion, x-ray temperature)
- Is a strong function of cosmology
- One of the main areas of research is to determine this function over a wide range in redshift.
- One of the main problems is relating observables to mass.

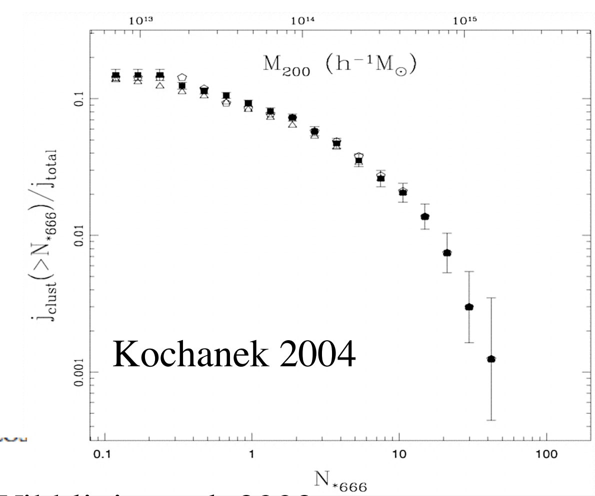

Kochanek 2004

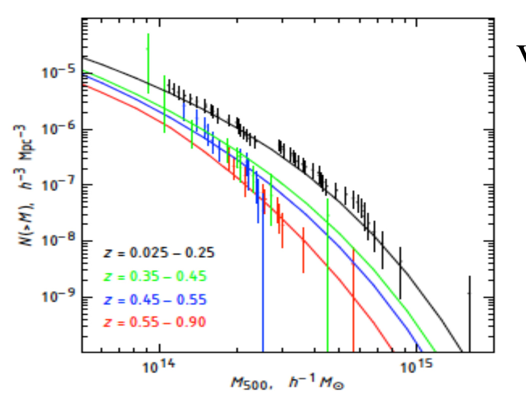

FIG. 18.— Same as Fig. 16 but the high-z sample is split into three redshift bins.

Vikhlinin et al 2009

The Galaxy Cluster Redshift Distribution

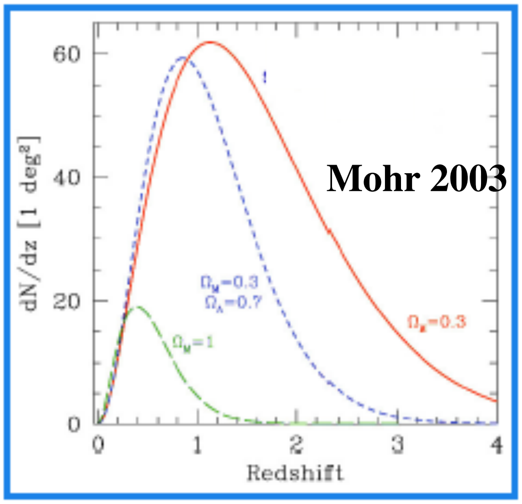

Redshift distribution of clusters in a flux limited survey for 3 sets of cosmological parameters

Cluster redshift distribution probes:

1) **volume-redshift relation**
2) **abundance evolution**
3) **cluster structure and evolution.**

f(M) contains the connections between the well understood theory of the formation of massive halos and the real world observations.

Mass Selection Function

$$\frac{dN(z)}{dz d\Omega} = \underbrace{\frac{dV}{dz\,d\Omega}}_{\text{Volume Element}} \underbrace{n(z)}_{\text{Abundance}} = \underbrace{\frac{c}{H(z)} d_A^2(1+z)^2}_{\text{Volume}} \underbrace{\int_0^\infty dM\, f(M) \frac{dn(M,z)}{dM}}_{\text{Abundance}}$$

Galaxy Cluster Abundance

Dependence on cosmological parameters

Haiman 2003

# of clusters per unit area and z:

$$\boxed{\frac{dN}{d\Omega dz}} = \underbrace{\frac{dV}{d\Omega dz}}_{\text{comoving volume}} \times \underbrace{\int_{M_{\min}}^{\infty}}_{\text{mass limit}} dM \underbrace{\frac{dn}{dM}}_{\text{mass function}}$$

mass function:

$$\frac{dn}{dM} = -0.315 \frac{\rho_0}{M} \left(\frac{1}{\sigma_M} \frac{d\sigma_M}{dM} \right) \exp\left\{ [0.61 - \log(g_z \sigma_M)]^{3.8} \right\}$$

Jenkins et al. 2001

overall normalization $(\propto \Omega_M h^2)$

power spectrum (σ_8, M-r) $(M \propto \Omega_M h^2 r^3)$

growth function

Hubble volume N-body simulations in three cosmologies cf: Press-Schechter

Relation of Velocity Dispersion and x-ray temperature

- The dispersion σ_r completely characterizes the radial velocity distribution function if it is Gaussian: $P(v_r)$ is the probability distribution of the velocity
- $P(v_r)=(1/\sigma_r \mathrm{sqrt}(2\pi))\exp(-(v_r-<v_r>)^2)/2\sigma^2_r$

the Gaussian velocity distribution in clusters suggests that they are at least partially relaxed systems, BUT they are not fully relaxed to thermodynamic equilibrium. In thermodynamic equilibrium, all components of the cluster would have equal temperatures; what is observed is that the velocity dispersion is nearly independent of galaxy mass

If relaxed the virial theorm says that $T\sim\sigma^2_r$

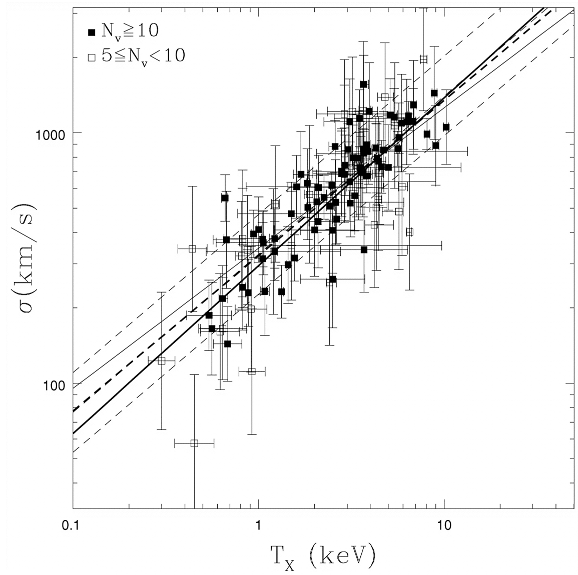

$$\log\left(\frac{\sigma}{10^3\ \mathrm{km\ s^{-1}}}\right) = (0.01 \pm 0.02) + (0.63 \pm 0.04)\log\left(\frac{T_X}{6\ \mathrm{keV}}\right), \quad (32)$$

Mass Estimation- Girardi et al 1998

In principle, one can estimate the cluster mass within a radius r, $M_J(<r)$, by using the Jeans equation, coupled with the equation which links the two observable quantities $\Sigma(R)$ and $\sigma_P(R)$, i.e. the projected galaxy number density and the projected velocity dispersion as a function of the projected radius R:

$$\frac{d(\rho\sigma_r(r)^2)}{dr} + \frac{2\rho(r)\beta\sigma_r^2}{r} = -\frac{G\rho(r)M_J(<r)}{r^2}, \quad (1)$$

$$\sigma_P^2(R)\Sigma(R) = 2\int_R^\infty \rho(r)\sigma_r^2(r)(1-\beta\frac{R^2}{r^2})\frac{r}{\sqrt{r^2-R^2}}dr \quad (2)$$

where r is the distance from the cluster center, $\rho(r)$ is the spatial number density of galaxies linked to $\Sigma(R)$ via the Abel integral, $\sigma_r(r)$ is the radial component of velocity dispersion $\sigma(r)$, and $\beta(r) = 1 - \sigma_\theta^2/\sigma_r^2$ is the velocity anisotropy parameter (e.g., Binney & Tremaine 1987).

Unfortunately, there are three unknowns ($M(<r)$,$\sigma(r)$, $\beta(r)$) and only two equations. In order to solve these equations it is therefore necessary to make some assumptions. It seems natural to assume knowledge of either $\beta(r)$ or $M(r)$, and then to evaluate the remaining two functions so that they are consistent to the observed velocity dispersion profile (e.g., Merritt 1987).

The virial theorem derives from the Jeans equation via an integration step. It relates the global kinetic energy with the potential one ($2T + U = 0$, e.g. Binney and Tremaine 1987) and is usually used to compute virial masses.

3.2 THE MASS DERIVED FROM THE VIRIAL THEOREM

The total virial mass of the cluster, M_V, depends on the global velocity dispersion, σ and the spatial distribution of the galaxy population (e.g., Merritt 1988):

$$M_V = \frac{<v^2>}{G<r^{-1}F>}, \quad (3)$$

where the brackets indicate spatial averages over the observed sample of N galaxies, r are the galaxy distances from the cluster center, and v are the galaxy velocities referred to the cluster mean velocity. The function $F(r)$ is the mass fraction within r and depends on the (generally) unknown form of mass distribution.

If mass is distributed like the observed galaxies (i.e., $\rho_{mass} \propto \rho$), then the appropriate form of eq. 3 is (Limber & Mathews 1960):

$$M_V = \frac{<v^2>}{G<r_{ij}^{-1}>} = \sigma^2 R_V/G \quad (4)$$

where R_V is the virial radius which depends on r_{ij}, i.e. the distance between any pair of galaxies.

From the observational point of view, the large advantage of the virial theorem is that the global projected velocity dispersion σ_P and, consequently, the total mass are independent of possible anisotropy of galaxy velocities, always being $\sigma^2 = 3\sigma_P^2$ for spherical systems (e.g., The & White 1986; Merritt 1988). Therefore, in the case of spherical systems, for the respective projected quantities σ_P and R_{PV}, eq. 4 becomes:

$$M_V = 3\pi/2 \cdot \frac{<V^2>}{G<R_{ij}^{-1}>} = 3\pi/2 \cdot \sigma_P^2 R_{PV}/G. \quad (5)$$

X-ray Mass Estimates

- use the equation of hydrostatic equilibirum
-

$$\frac{dP_{\rm gas}}{dr} = \frac{-G\mathfrak{M}_*(r)\rho_{\rm gas}}{r^2} \qquad (3)$$

where $P_{\rm gas}$ is the gas pressure, $\rho_{\rm gas}$ is the density, G is the gravitational constant, and $\mathfrak{M}_*(r)$ is the mass of M87 interior to the radius r.

$$P_{\rm gas} = \frac{\rho_{\rm gas} K T_{\rm gas}}{\mu \mathfrak{M}_{\rm H}} \qquad (4)$$

where μ is the mean molecular weight (taken to be 0.6), and $\mathfrak{M}_{\rm H}$ is the mass of hydrogen atom.

$$\frac{KT_{\rm gas}}{\mu\mathfrak{M}_{\rm H}}\left(\frac{d\rho_{\rm gas}}{\rho_{\rm gas}} + \frac{dT_{\rm gas}}{T_{\rm gas}}\right) = \frac{-G\mathfrak{M}_*(r)}{r^2}dr, \qquad (5)$$

which may be rewritten as:

$$-\frac{KT_{\rm gas}}{G\mu\mathfrak{M}_{\rm H}}\left(\frac{d\log\rho_{\rm gas}}{d\log r} + \frac{d\log T_{\rm gas}}{d\log r}\right) r = \mathfrak{M}_*(r) \qquad (6)$$

Putting numbers in gives

$$M(r) = -3.71\times10^{13}\,M_\odot\,T(r)\,r\left(\frac{d\log\rho_g}{d\log r} + \frac{d\log T}{d\log r}\right),$$

ere T is in units of keV and r is in units of Mpc. (

$$\frac{n_0^2}{(1+r^2/r_c^2)^{3\beta}}$$

VIKHLININ ET AL.

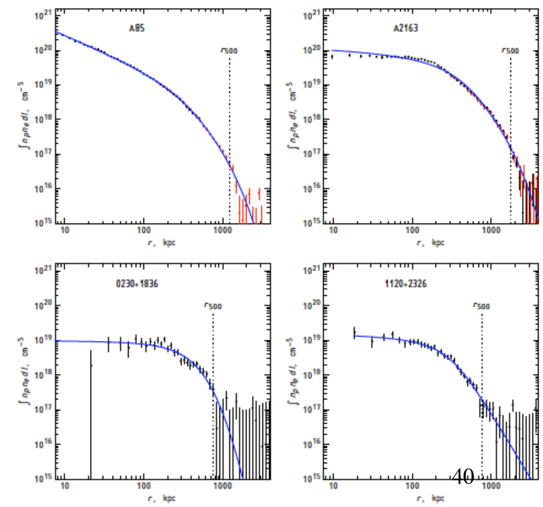

FIG. 5.— Examples of the surface brightness profile modeling for clusters shown in Fig. 3 and 4. The observed X-ray count rates are converted to the projected emission measure integral (see § 3.4 and V06). The black and red data points show the *Chandra* and *ROSAT* measurements, respectively. The best fit models (the projected emission measure integral for the three-dimensional distribution given by eq. 2) are shown by solid lines. The dashed lines indicate the estimated r_{500}

Intracluster Gas

- **Majority (75%) of observable cluster mass (majority of baryons) is hot gas**
- **Temperature $T \sim 10^8$ K ~ 10 keV**
- **Electron number density $n_e \sim 10^{-3}$ cm^{-3}**
- **Mainly H, He, but with heavy elements (O, Fe, ..)**
- **Mainly emits X-rays**
- **$L_X \sim 10^{45}$ erg/s, most luminous extended X-ray sources in Universe**
- **Age ~ 2-10 Gyr**

Sarazin

The Intracluster Medium as a Fluid

$$\lambda_p \approx \lambda_e = \frac{3^{3/2}(kT)^2}{8\sqrt{\pi}\, n_e e^4 \ln\Lambda}$$

$$\approx 23 \left(\frac{T}{10^8\ \mathrm{K}}\right)^2 \left(\frac{n_e}{10^{-3}\ \mathrm{cm}^{-3}}\right)^{-1} \mathrm{kpc}$$

Mean-free-path $\lambda_e \sim 20$ kpc $< 1\%$ of diameter $\rightarrow$ fluid
(except possibly in outer regions, near galaxies, or at shocks and cold fronts)

Sarazin

Physical State of Intracluster Gas: Local Thermal State

- **Mainly ionized, but not completely**
- **Coulomb collision time scales**

  τ(e,e) ~ 10^5 yr
  τ(p,p) ~ 4 x 10^6 yr
  τ(p,e) ~ 2 x 10^8 yr
  all < age (>10^9 yr)

  Kinetic equilibrium, Maxwellian at T
  Equipartition T_e=T_p
  (except possibly at shocks)

X-ray Emission Processes

- **Continuum emission**
  - **Thermal bremsstrahlung, ~exp(-hν/kT)**
  - **Bound-free (recombination)**
  - **Two Photon**
- **Line Emission**

  (line emission)

  $L_\nu \propto \varepsilon_\nu\ (T, \text{abund})\ (n_e^2\ V)$

  $I_\nu \propto \varepsilon_\nu\ (T, \text{abund})\ (n_e^2\ l)$

X-ray Spectrum

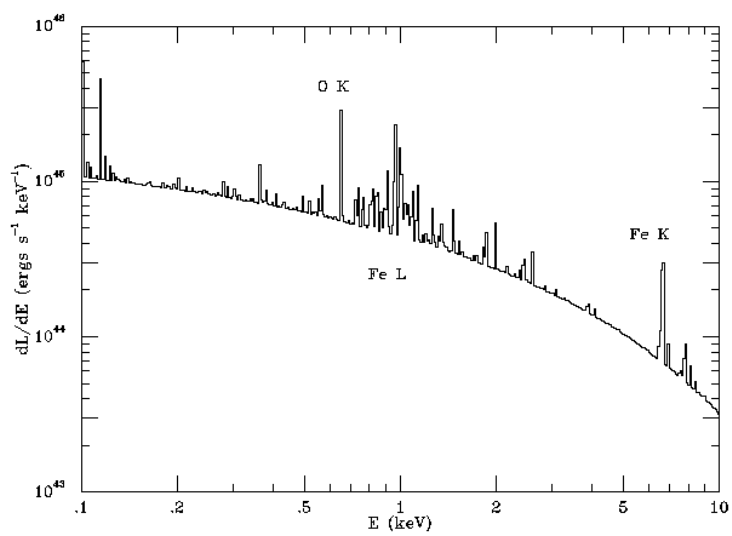

The Intracluster Medium as a Fluid (cont.)

- **Specify local:**
  - **Density (ρ or n_e)**
  - **Pressure P**
  - **Internal energy or temperature T**
  - **Velocity v**
- **Ideal gas $P = n\,k\,T$**

(except for nonthermal components; cosmic rays, magnetic fields)

Magnetic Fields in Clusters

$B \sim \mu G \rightarrow P_B \ll P_{gas}$ in general in clusters

Electron, ions gyrate around magnetic field lines

$r_g \approx 10^8$ cm « scales of interest

- **Act like effective mean free path, make ICM more of a fluid**
- **Suppress transport properties $\perp$ B**
  Could greatly reduce thermal conduction, but depends on topology of B fields

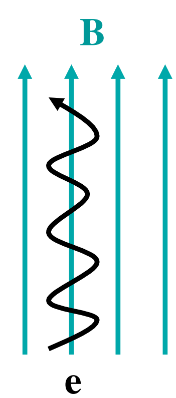

Heating and Cooling of ICM

- **What determines temperature T?**
- **Why is ICM so hot?**
- **What are heating processes?**
  - **gravitational heating**
  - **nongravitational heating (SNe, AGNs)**
- **What are cooling processes?**

Sarazin

Why is gas so hot?

- Clusters have huge masses, very deep gravitational potential wells
- Any natural way of introducing gas causes it to move rapidly and undergo fast shocks

infall

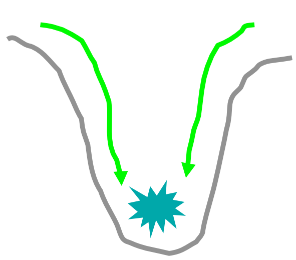

galaxy ejection

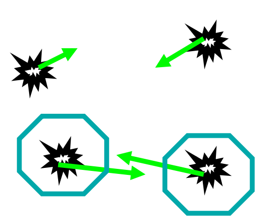

All intracluster gas is shocked at ~2000 km/s

Cluster Mergers

Clusters from hierarchically, smaller things form first, gravity pulls them together

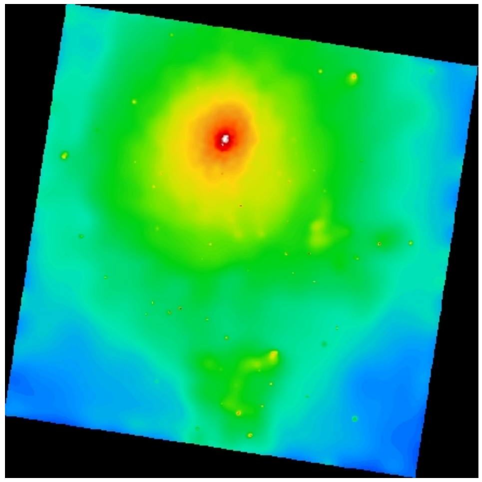

Abell 85 Chandra

Merger Shocks

⇨ **Main heating mechanism of intracluster gas**

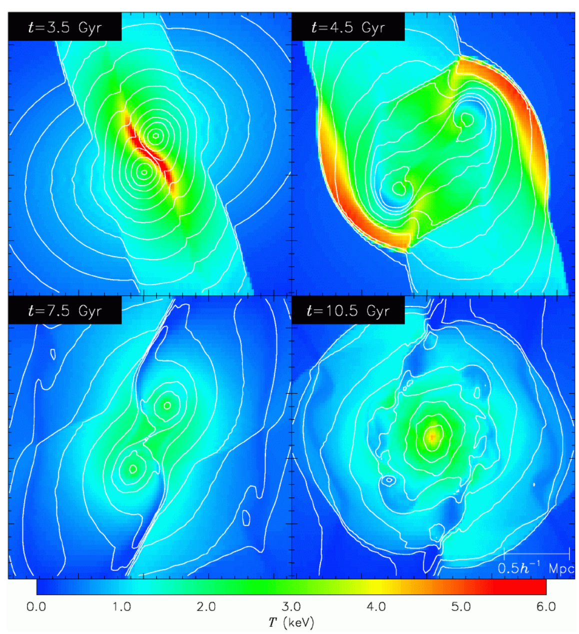

Simple Scaling Laws for Gravitational Heating (Kaiser 1986)

- Gas hydrostatic in gravitational potential
  $kT \sim \mu m_p \, GM/R$
- Clusters formed by gravitational collapse
  $\langle \rho_{cluster} \rangle \sim 180 \, \rho_{crit} \, (z_{form})$
- Most clusters formed recently, $z_{form} \sim$ now
- Baryon fraction is cosmological value, most baryons in gas
  $R \propto (M / \rho_{crit}^{0})^{1/3} \propto M^{1/3}$
  $T \propto M^{2/3}$
  $L_X \propto T^2$

Radiative Cooling of ICM

- Main cooling mechanism is radiation, mainly X-rays

  $L = \Lambda(T,\text{abund}) \, n_e^2$
  ergs/cm^3/s

  $T \gtrsim 2$ kev, $\Lambda \propto T^{1/2}$
  Thermal bremsstrahlung
  $T \lesssim 2$ keV, $\Lambda \propto T^{-0.4}$
  X-ray lines

Very important in high density regions-center of cluster, 'cooling flows'

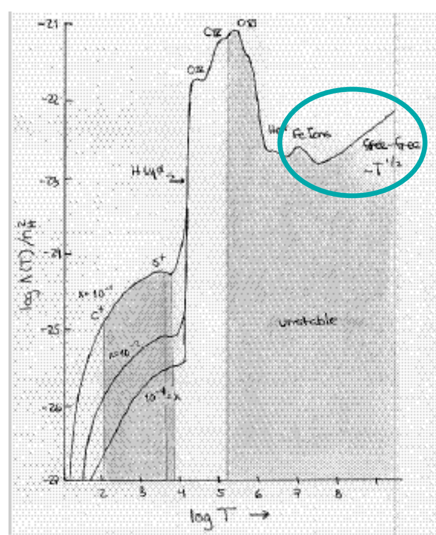

Radiative Cooling (cont.)

- **Cooling time (isobaric, constant pressure)**

$$\Rightarrow \quad t_{cool} = 69\left(\frac{n_e}{10^{-3}\,\mathrm{cm}^{-3}}\right)^{-1}\left(\frac{T}{10^{8}\,\mathrm{K}}\right)^{1/2}\mathrm{Gyr}$$

- **Longer than Hubble time in outer parts of clusters**
- **Short in centers of ~1/2 clusters, "cooling flows", $t_{cool} \sim 3 \times 10^8$ yr**

Heating of ICM - Summary

- **Most of energy in large clusters due to gravity, mergers of clusters**
- **Smaller clusters, groups, centers of clusters → significant evidence of nongravitational heating**
- **Due to galaxy and star formation, supernovae, formation of supermassive BHs**

  ICM/IGM records thermal history of Universe

Sarazin

Sound Crossing Time

- **Sound speed** $$c_s^2 = \gamma \frac{P}{\rho} = \frac{5}{3}\frac{P}{\rho}$$

$$c_s \approx 1500 \left(\frac{T}{10^8\,\mathrm{K}} \right)^{1/2} \mathrm{km/s}$$

- **Sound crossing time**

$$t_s \approx 6.6 \times 10^8 \left(\frac{T}{10^8\,\mathrm{K}} \right)^{-1/2} \left(\frac{D}{\mathrm{Mpc}} \right) \mathrm{yr}$$

Less than age → unless something happens (merger, AGN, …),
gas should be nearly hydrostatic

- **Sarazin**

Hydrostatic Equilibrium

$$\nabla P = -\rho \nabla \phi$$

$$\frac{1}{\rho}\frac{dP}{dr} = -\frac{d\phi}{dr} = -\frac{GM(r)}{r^2} \quad \text{spherical}$$

Isothermal (T = constant)

$$\frac{1}{\rho}\nabla P = \frac{1}{\rho}\nabla\left(\frac{\rho k T}{\mu m_p} \right) = \left(\frac{kT}{\mu m_p} \right) \nabla \ln \rho = -\nabla \phi$$

$$\ln\left[\rho(r) \big/ \rho_0 \right] = \left(\frac{\mu m_p}{kT} \right) \left[\phi_0 - \phi(r) \right]$$

Cluster Potentials

NFW **(Navarro, Frenk, & White 1997)**

$$\rho_{dm}(r) = \frac{\rho_s}{\frac{r}{r_s}\left(1+\frac{r}{r_s}\right)^2}$$

$c \equiv r_{vir}/r_s \approx 5$ for clusters,

$r_{vir} \approx 2\,\text{Mpc},\ \ r_s \approx 400\,\text{kpc}$

$$M(r) = 4\pi\rho_s r_s^3\left[\ln(1+\frac{r}{r_s}) - \frac{r}{r+r_s}\right]$$

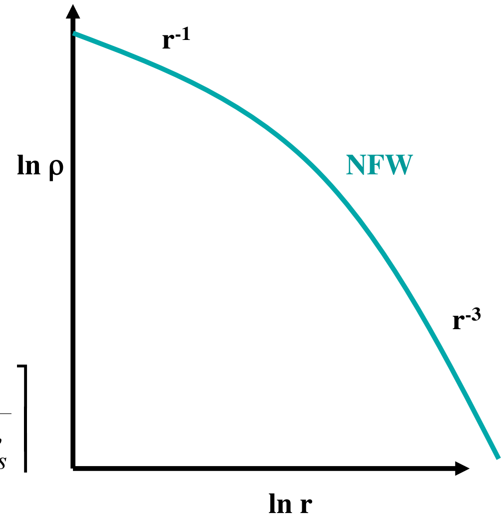

Cluster Potentials (cont.)

Analytic King Model (approximation to isothermal sphere

$$\rho_{dm}(r) = \frac{\rho_{dm,0}}{\left[1+\left(\frac{r}{r_c}\right)^2\right]^{3/2}}$$

$r_c \approx r_s/2 \approx 200\,\text{kpc}$

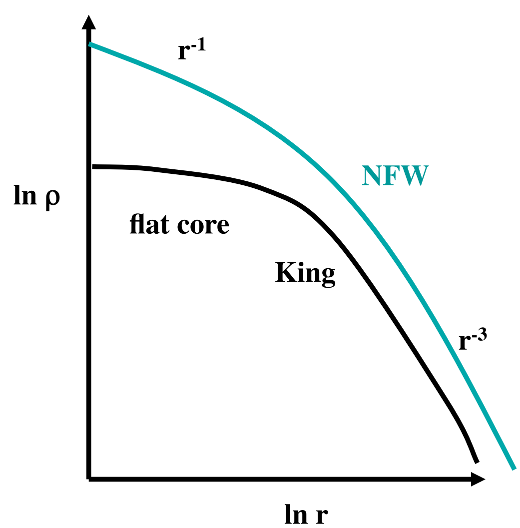

Beta Model

(Cavaliere & Fusco-Femiano 1976)

Assume King Model DM potential Alternatively, assume galaxies follow King Model, and have isotropic, constant velocity dispersion

$$\sigma_{gal}^2 \frac{d \ln \rho_{gal}}{dr} = -\frac{d\phi}{dr} = \left(\frac{kT}{\mu m_p}\right)\frac{d \ln \rho}{dr}$$

$$\rho_{gal}(r) = \frac{\rho_{gal,0}}{\left[1 + \left(\frac{r}{r_c}\right)^2\right]^{3/2}}$$

Beta Model (cont.)

$$\rho(r) = \frac{\rho_0}{\left[1 + \left(\frac{r}{r_c}\right)^2\right]^{3\beta/2}}$$

$$\beta \equiv \frac{\mu m_p \sigma_{gal}^2}{kT} \text{ but treat as fitting parameter}$$

$$I_X(r) \propto \left[1 + \left(\frac{r}{r_c}\right)^2\right]^{-3\beta+1/2}$$

Where do the Baryons Go?

- Most of the baryons in the universe (>80%) do not live in galaxies (Fukugita and Peebles 2007) Ω_{stars} h = 0.0027 +/- 0.00027

Ω_{total}(Baryon)h^2 =0.0214

- In a simulation of the formation of structure only a small fraction of the baryons (light blue) end up as stars

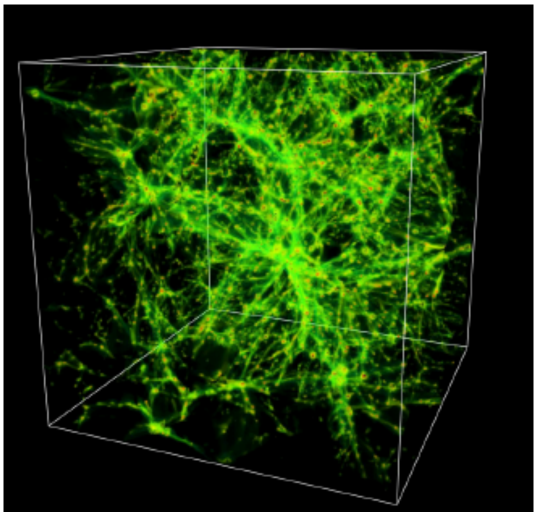

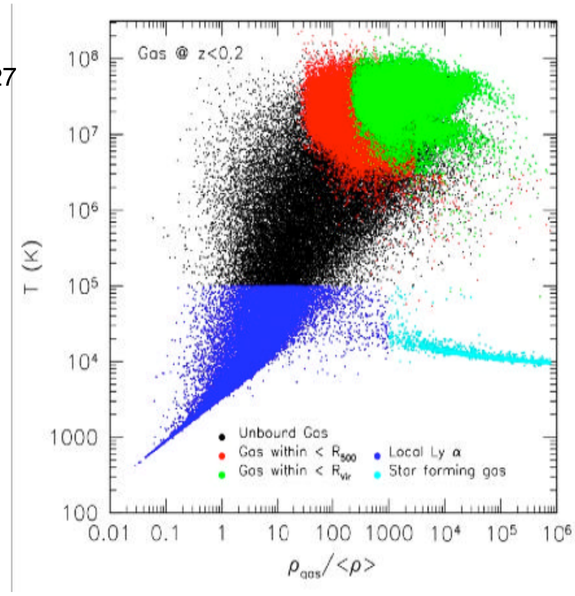

Particles in red and green are in clusters- red closer to center

How to Measure the Mass and Baryonic Mass of a System

- Measure its light and from stellar evolution theory transform light to mass.
- This is most accurate in the near-IR (K band) - if one includes all the objects which once were main sequence stars (e.g. white dwarfs, neutron stars, black holes) there is a factor of 2 theoretical error (e.g. M/L_K(solar units) ~0.8-1.9 (Ellis 2009)
- One can actually measure this in a wide range of objects using the dynamics of stars to get the total mass of the galaxy (Bell et al 2007(

Basics of Gravitational Lensing

- See Lectures on Gravitational Lensing by

Ramesh Narayan Matthias Bartelmann or
 http://www.pgss.mcs.cmu.edu/1997/Volume16/physics/GL/GL-II.html

For a detailed discussion of the problem

- Rich centrally condensed clusters occasionally produce giant arcs when a background galaxy happens to be aligned with one of the cluster caustics.
- ***Every cluster*** produces weakly distorted images of large numbers of background galaxies.
  - These images are called arclets and the phenomenon is referred to as weak lensing.

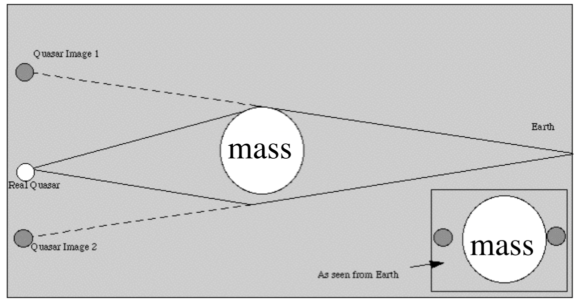

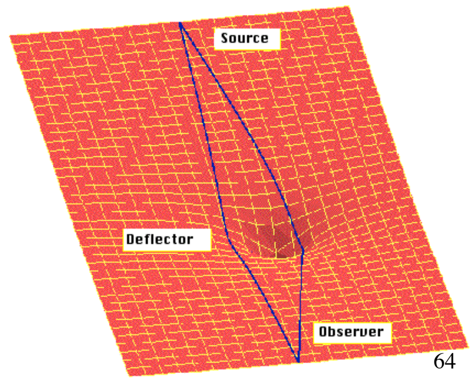

64

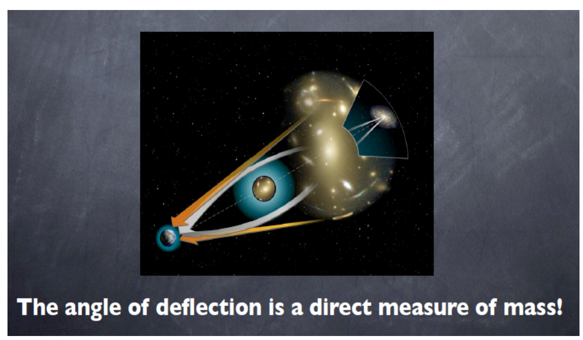

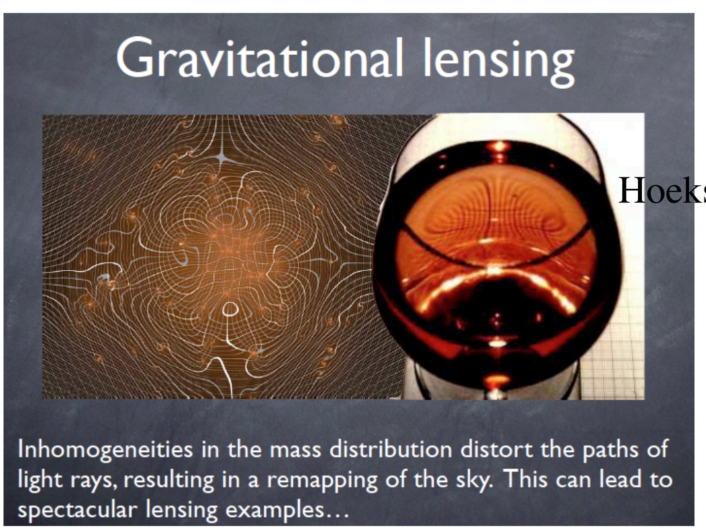

Hoekstra 2008 Texas Conference

65

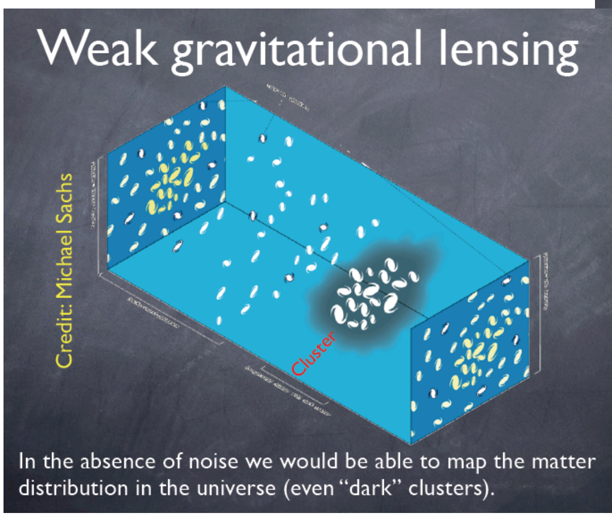

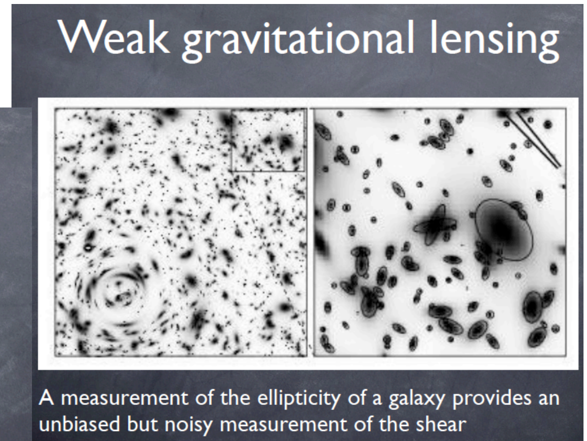

Hoekstra 2008 Texas Conference

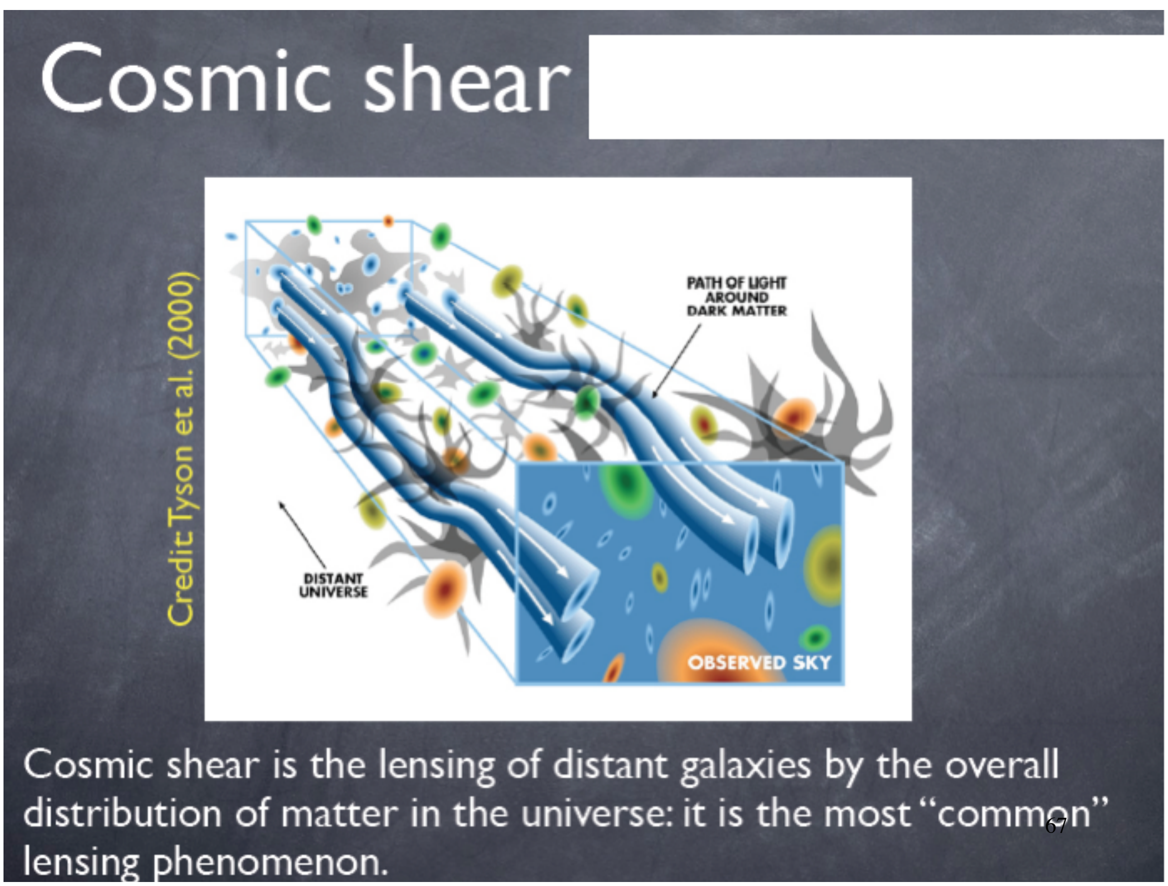

The Sunyaev-Zel'dovich Effect: probe of Galaxy clusters

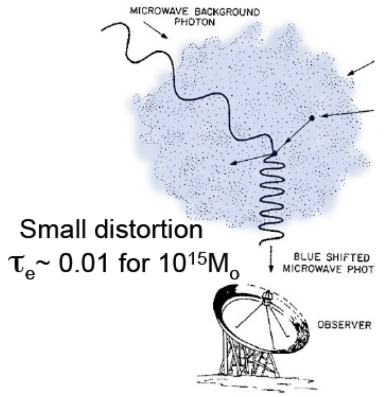

from Leon Van Speybroeck

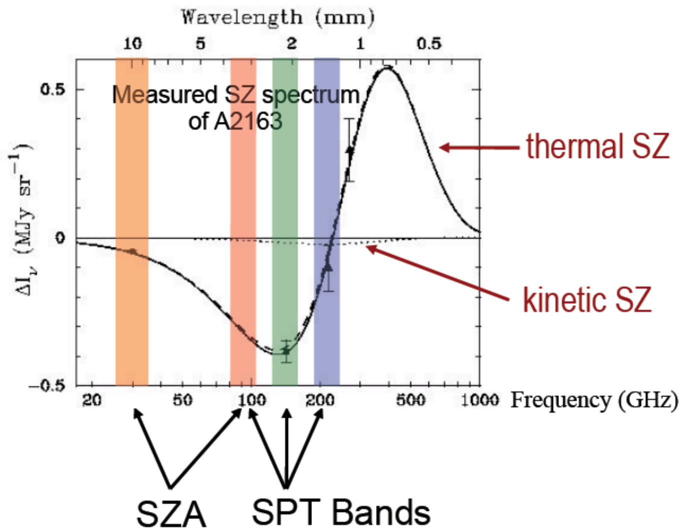

Carlstrom

Redshift independent: $\frac{\Delta T_{SZE}}{T_{CMB}} \propto \int n_e T_e dl$

The beauty of the SZ Effect

Thermal SZE is a small (<1 mK) distortion in the CMB caused by inverse Compton scattering of the CMB photons

$$\frac{\Delta T}{T_{\rm CMB}} = g(x) \int n_e(l)\, \frac{k_{\rm B} T_e(l)}{m_e c^2}\, dl$$

Total cluster flux density is independent of redshift!

$$\Delta S_\nu = \int \Delta I_\nu \, d\Omega \propto \frac{\int n_e T_e \, dV}{D_{\rm A}^2} \propto \frac{f_{\rm gas} M_{\rm tot} T_e}{D_{\rm A}^2}$$

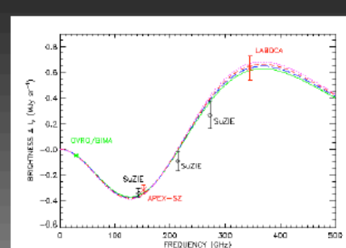

Nord, Basu, Pacaud et al, 2009

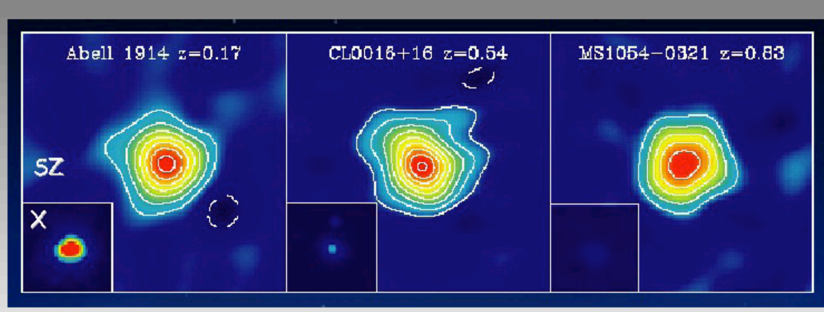

Carlstrom et al.

Sunyaev-Zel'dovich Effect

Single Clusters

- *Measure of integrated pressure (total thermal energy)*
- *Distances, H_o, $H(z)$*
- *Cluster gas mass fractions, cluster structure, evolution studies*
- *Peculiar velocities at high z*

$$\boxed{\frac{\Delta T_{SZE}}{T_{CMB}} \propto \int n_e T_e dl}$$

SZ Cluster Surveys

NEW

- *Exploit SZ redshift independence*
- *Measure growth of structure and large scale velocity fields to constrain Dark Energy*

$$\boxed{\begin{aligned} S &\propto \int \Delta T_{SZE}\, d\Omega \\ &\propto \frac{1}{D_A(z)^2} \int n_e T_e dV \end{aligned}}$$

Carlstrom

S-Z Simple Physics

- The optical depth for the S-Z effect is small
- the density of electrons is of order $n_e \sim 10^{-3}$ cm^{-3}, the path length ` through a cluster medium ~ several Mpc. With a Thomson cross section σ= 6.65 x10 $^{-25}$ cm^2,

optical depth $\tau = n_e \sigma l \sim 0.005$; ~ 1%

probability that a CMB photon crossing a rich cluster is scattered by an electron.

- Since the electron energy is much larger that the energy of the photon, to first order $\delta\nu/\nu \sim kTe/m_e c^2 = 1\%$. The resulting fractional temperature change of the CMB is of the order of 10^{-4},~300µk
- For a review see *Carnegie Observatories Astrophysics Series, Vol. 3: Clusters of Galaxies: Probes of Cosmological Structure and Galaxy Evolution, 2004* Using the Sunyaev-Zelídovich Effectto Probe the Gas in Clusters MARK BIRKINSHAW

The spectrum of the thermal SZE has a characteristic shape
all interacting CMB photons get approximately a 1% boost in energy, the result is a transfer of photons in the CMB spectrum from lower to higher frequencies, resulting in a decrease of brightness at low frequencies

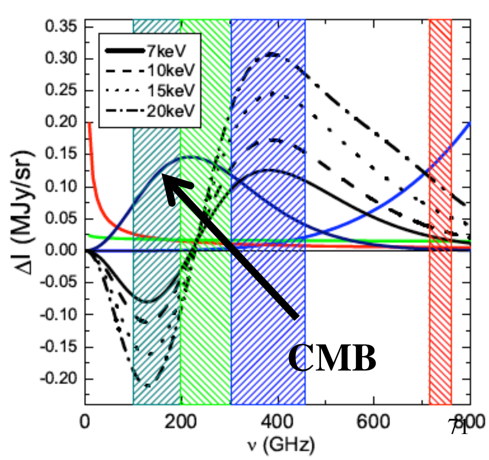

A Strange Fact

- As clusters are observed at higher redshifts the solid angle which scatters the CMB gets smaller- however the CMB gets brighter in the past
- These two terms almost cancel IF the cluster hot gas were the same at higher redshifts.
- Since we expect the cluster hot gas to evolve with z it is not clear what the total effect will be .
- The amplitude of the S-Z effect is t independent of D_A the angular distance

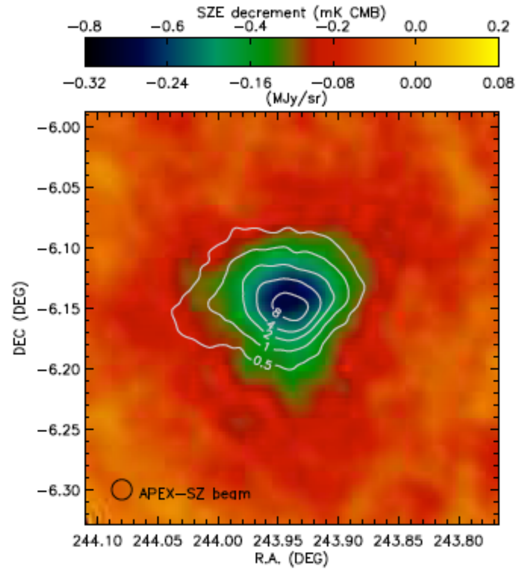

Fig. 1. Map of Abell 2163 at 150 GHz, overlaid with XMM-Newton X-ray contours (see Fig. 3) in units of 10^{-13} erg s^{-1}cm^{-2}arcmin^{-2}. Because the correlated-noise re-

Sunyaev-Zeldovich Distances

- The Sunyaev-Zeldovich effect is the Compton scattering of microwave background photons off the hot electrons in the IGM in the cluster
- At present ~400 clusters have measured S-Z effect "decrements" and x-ray temperatures (Primarily from Planck and the South Pole Telescope and the Atacama Cosmology telescope)

Line integral of pressure

$$\Delta T \propto g(\nu) \int dz\, n_e(\mathbf{r})\, T_e(\mathbf{r}),$$

$$S_X \propto \frac{1}{(1+z)^4} \int dz\, n_e(z)^2\, T_e(z)\, \Lambda(T_e, Z_{ab}),$$

Geometry uncertainty

$$H_0 \propto \left(\frac{T_e}{\Delta T_{SZ}}\right)^2 \theta S_X \frac{\ell_\perp}{\ell_\parallel},$$

$$D_A \propto \frac{(\Delta T_0)^2 \Lambda_{eH0}}{S_{x0} T_{e0}^2} \frac{1}{\theta_c},$$

Angular distance D_A:ΔT_0 is the S-Z decrement, S_{X0} the x-ray surface brightness, T_{e0} the x-ray temperature,θ an angular size and Λ the cooling function

All quantities are directly measurable with an x-ray image, temperature map and S-Z image

Sunyaev-Zeldovich effect

- Compton scattering changes both the angular and energy distribution of the microwave background
- At low frequencies the result is a diminution (decrement) in the surface brightness of the MWB whose amplitude and shape depends on the Compton optical depth, the 3-D distribution of the hot electrons and their temperature

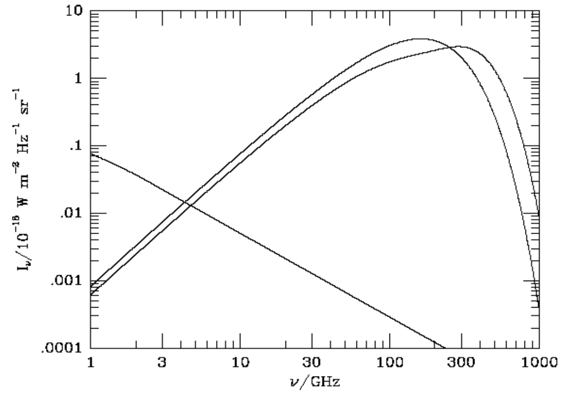

Fig. 1.— The spectrum of the microwave background radiation, and the microwave background radiation after passage through an (exaggerated) scattering atmosphere with $y = 0.1$ and $\tau\beta = 0.05$ (as defined in Sections 3 and 6), compared with the integrated

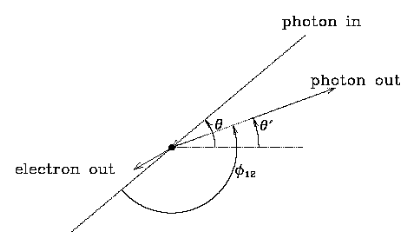

— The scattering geometry, in the frame of rest of the electron before the interaction. ...oming photon, at angle θ relative to the x_e axis, is deflected by angle ϕ_{12}, and emerges

Sunyaev-Zeldovich effect

- The main technical limits are the long exposures required in both the x-ray band and the milli-meter (~1 day each for the highest z clusters)
- The S-Z decrement is independent of redshift, while the x-ray surface brightness drops as $(1+z)^4$

  Setting a practical limit to z~1.3 for the x-ray measurements
- In a massive cluster the typical optical depth is τ ~0.1

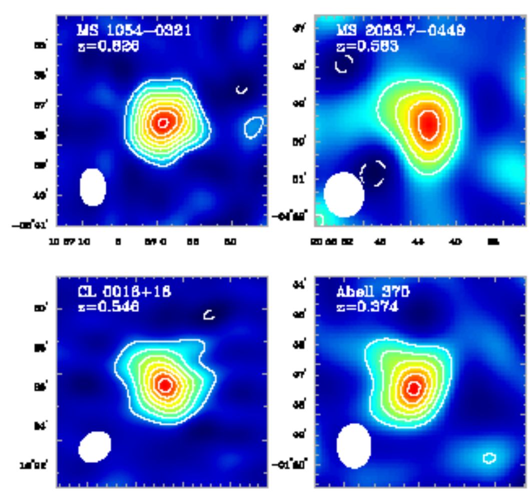

S-Z contours images for a sample of clusters from z~0.3-0.9

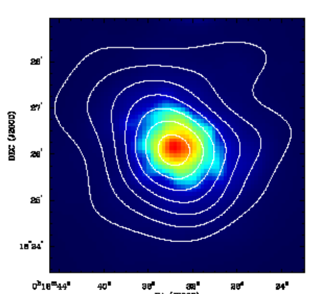

X-ray image with S-Z contours for z=0.54 cluster

Clusters of Galaxies an X-ray Perspective

Probes of the history of structure formation

Dynamical timescales are not much shorter than the age of the universe

• Studies of their evolution, temperature and luminosity function can place strong constraints on all theories of large scale structure

• and determine precise values for many of the cosmological parameters

Provide a record of nucleosynthesis in the universe- as opposed to galaxies, clusters probably retain all the enriched material created in them

•Measurement of the elemental abundances and their evolution provide fundamental data for the origin of the elements

•The distribution of the elements in the clusters reveals how the metals were removed from stellar systems into the IGM

Clusters should be "fair" samples of the universe"

•Studies of their mass and their baryon fraction reveal the "gross" properties of the universe as a whole

•Much of the entropy of the gas in low mass systems is produced by processes other than shocks-

- a major source of energy in the universe ?
- a indication of the importance of non-gravitational processes in structure formation ?

Origin of 'Metals'

- Metal production is dominated for (0…Ni) by supernova.
- Type II (core collapse) produce most of the O and Type I produce most of the Fe.
- The fraction of other elements (e.g. Si,S) that are produced by the SN depend on the IMF and the (poorly understood) yields of the SN.
- If the observed cluster galaxiesare the source of the metals and 'standard' SN rates and IMF are assued (Portinari et al 2004) then one cannot produce the observed metals
- One is led to either non-standard IMFs, a strong evolution in SN (which is now being constrained) or another source of metals (stars in the IGM

In any case >70% of the metals generated in galaxies has to be 'lost' to the ICM and
A factor of 3 high SN rate in clusters than in the field

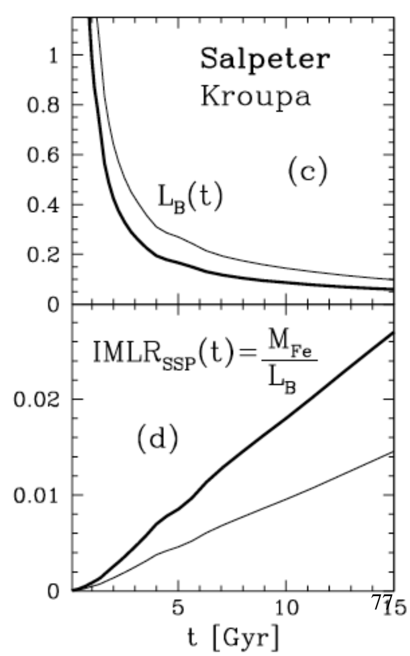

Metals in Clusters

- One of the main issues in cluster physics is when and how the metals in the ICM are created
- Pattern of metallicity
- Evolution of metallicity
- Simple numbers
- Feedback

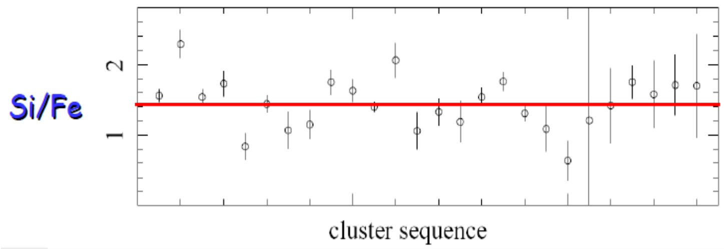

1.47 ± 0.05

$\sigma_{Si/Fe} \sim 20\%$

The Si, Fe, Ni abundances as well as Si/Fe and Ni/Fe abundance ratios distributions of the sample show moderate spread (from 20% to 30%)

Molendi et al 2009

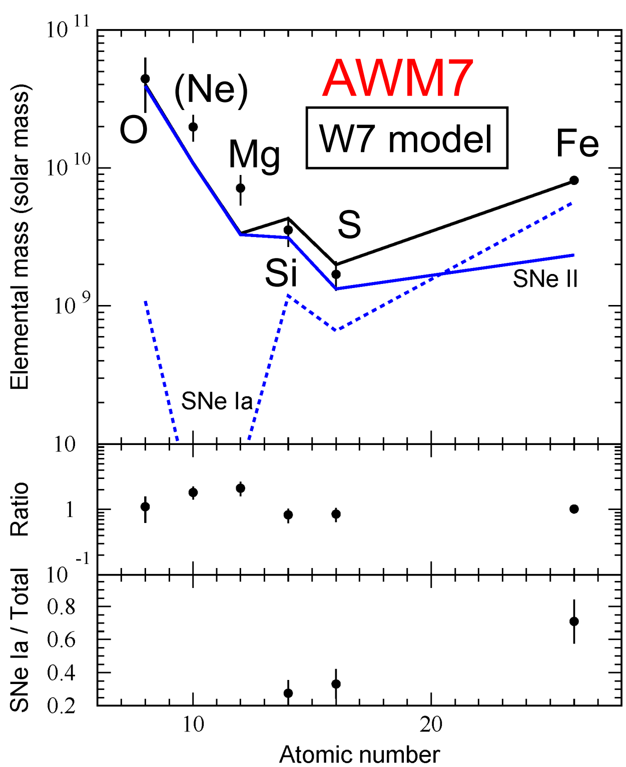

χ^2 / dof
= 15.9 / 3

$N_{\mathrm{SNe\ II}} / N_{\mathrm{SNe\ Ia}}$
= 4.0 ± 1.2

- ~75% of Fe, ~40% of Si and S from SNe Ia

Sato et al

Pattern of metals

- Pattern of metals compared to a model consisting of a sum of TypeI and Type II SN- relative amounts are a free parameter

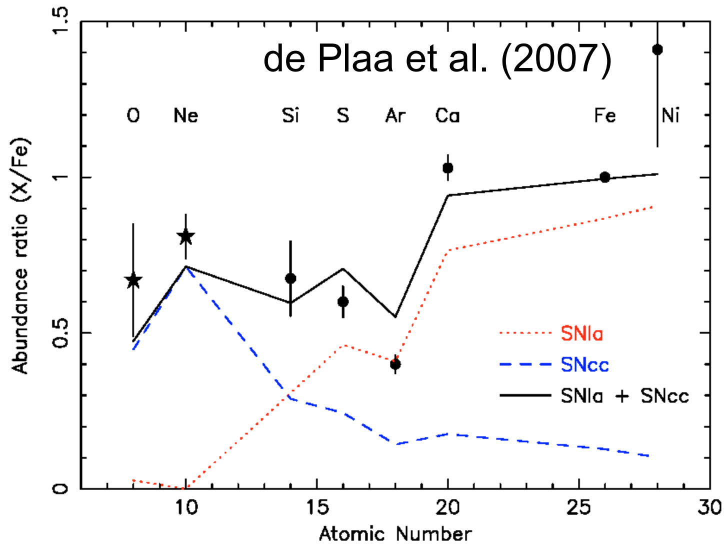

Numbers and Ratio of SNe Ia &

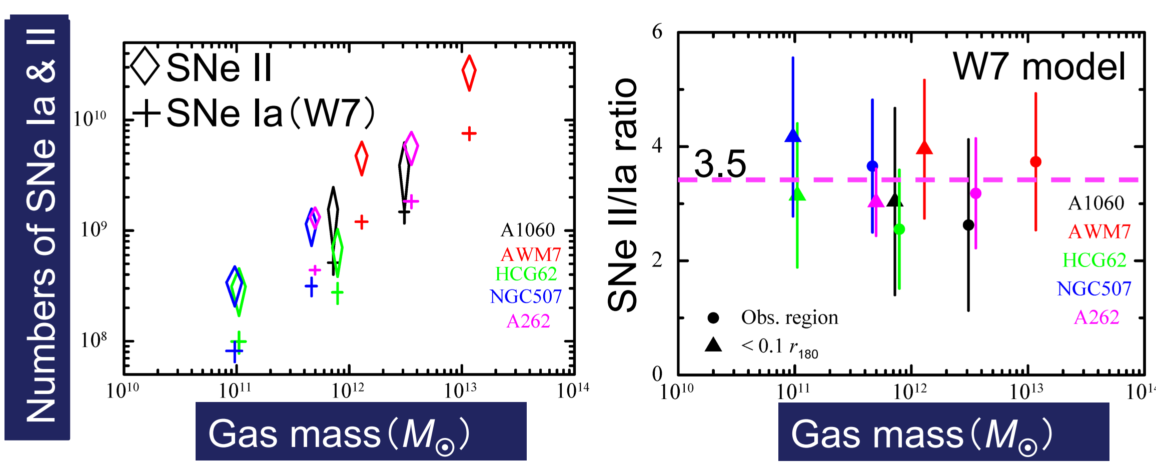

- Numbers of SNe Ia &
  SNe II/Ia Ratio: ~3.5 (W7 and WDD2), ~2.5 (WDD1)

cf. Clusters (*XMM* ; de Plaa et al. 2007): ~3.5
Our Galaxy (Tsujimoto et al. 1995): ~6.7
LMC & SMC (Tsujimoto et al 1995): 3.3 – 5

Metallicity Evolution

- There is weak evidence for cluster metallicity evolution- however sample selection effects may dominate
- Most of the metals were in place at z~0.5 and maybe at z~1

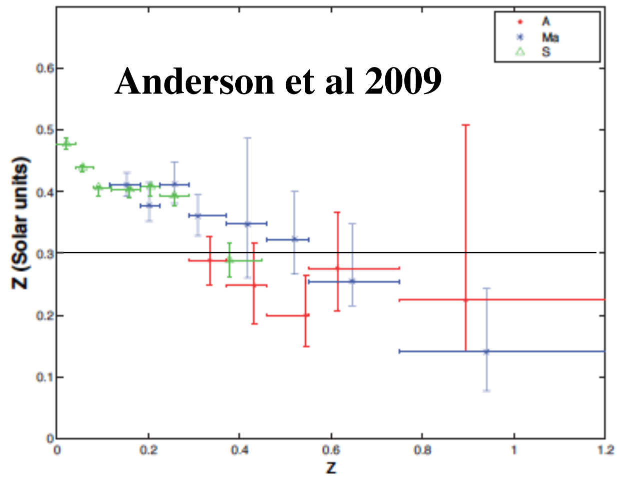

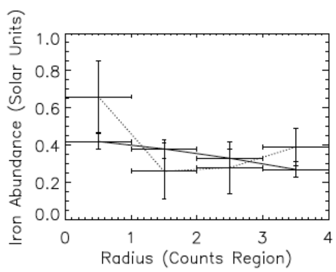

Fig. 2. Iron abundance as a function of radius for clusters with high temperatures and short cooling times, separated by redshift. The solid line corresponds to subset # 2 ($z < 0.4$). The dashed line corresponds to subset # 6 ($z > 0.4$).

Ehlert and Ulmer 2009

Metals are synthesized in stars (galaxies):
Compare $M_{\mathrm{metal}, < R}$ (in units of $\boldsymbol{M_\odot}$)
with stellar luminosity

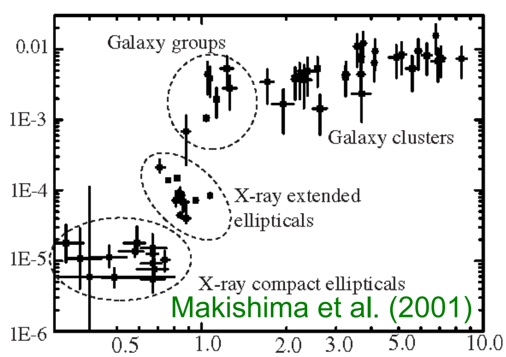

Temperature (keV) $\propto$ mass of system

$$\mathbf{MLR} = \frac{\boldsymbol{M}_{\mathbf{metal}, < \boldsymbol{R}}}{\boldsymbol{L}_{\mathbf{B\ or\ K}, < \boldsymbol{R}}} \quad \frac{\boldsymbol{M_\odot}}{L_\odot}$$

Oxygen Mass-to-Light Ratio: OMLR
Magnesium Mass-to-Light Ratio: MMLR
Iron Mass-to-Light Ratio: IMLR

Metal enrichment process in the ICM
- shows factor of several variation

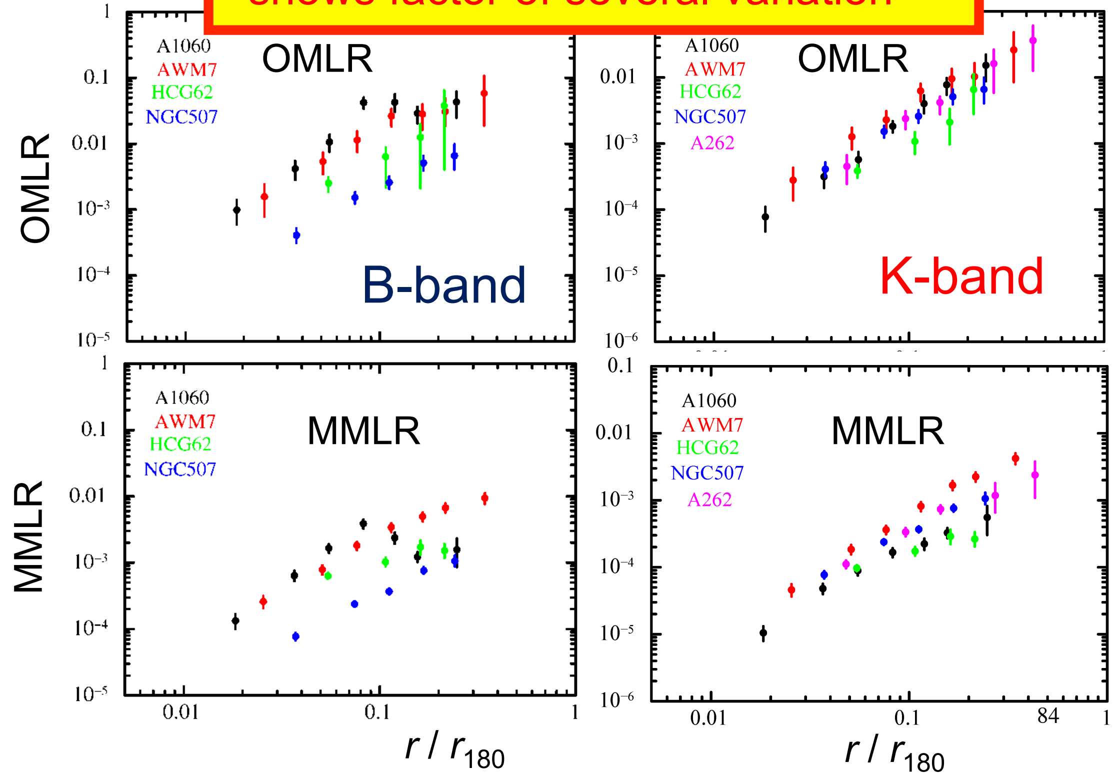

Comparison of Numbers of SNe II

Number of SNe II expected from Star Formation Rate of Hubble Deep Field (Madau et al. 1998)

➢ Numbers of SNe II expected from the metal mass observed with *Suzaku*

Normalized by K-band（2MASS）luminosities

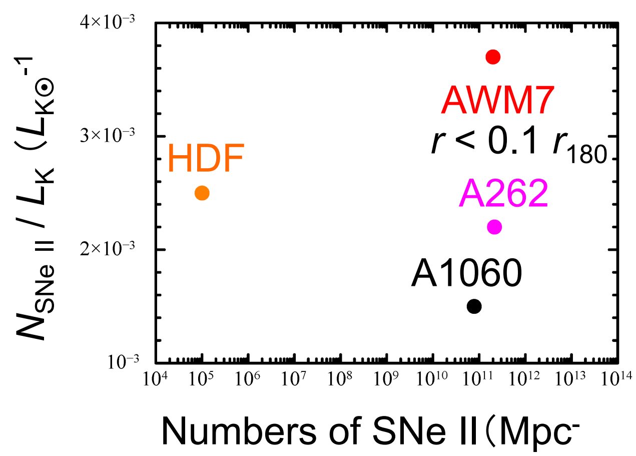

$N_{SNe\ II}$ normalized by L_K between field galaxy and clusters from our obs.

Feedback- How AGN Influence the Cluster Gas

Direct evidence from cluster x-ray images combined with radio data that central AGN has strongly influenced the gas

86

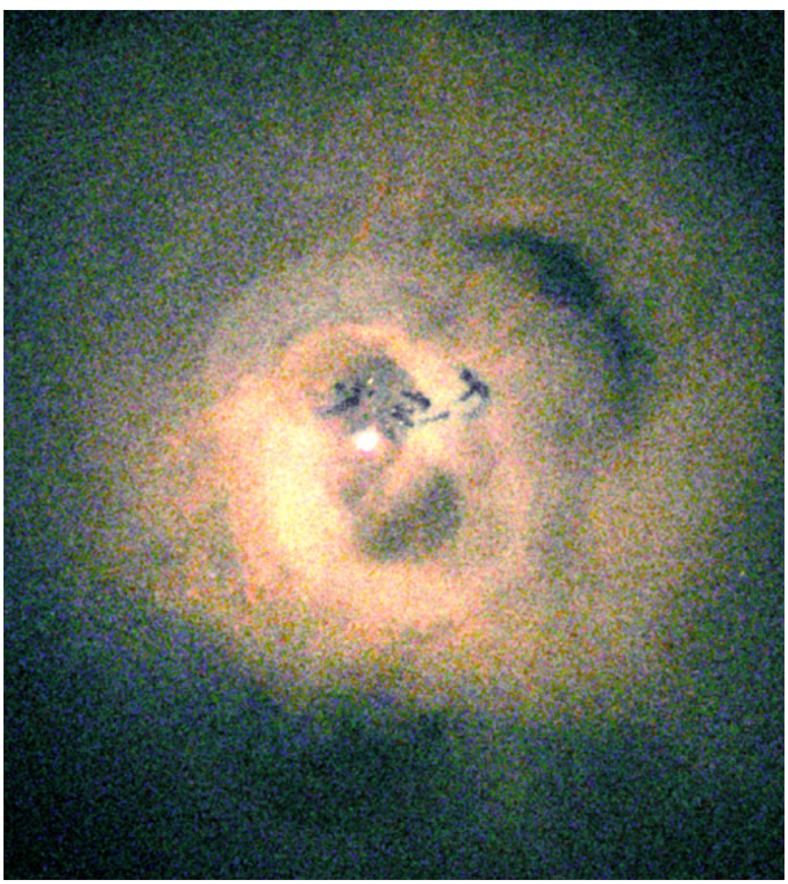

Jet power
= feedback?

87

Cavaties and Low Freq Radio Emisson

- The giant cavaties seen in many cooling flow clusters are often 'filled' by low frequency radio emitting plasama

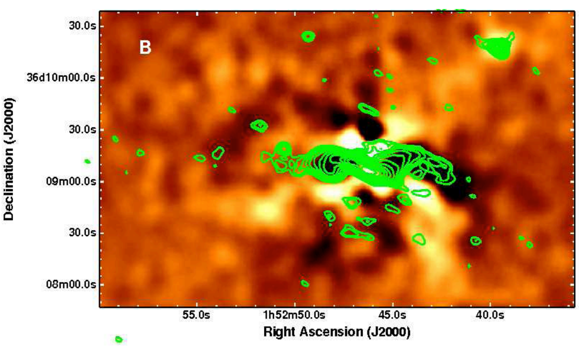

A262 Clarke et al 2009

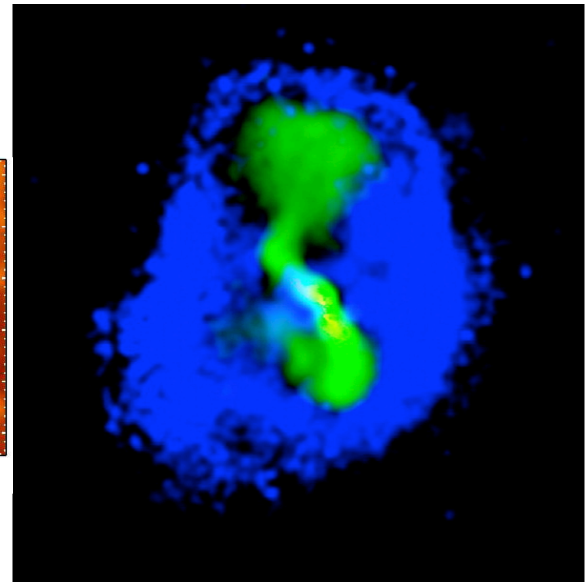

Hydra A Wise et al 2007

Effects of Feedback in Image and Temperature

the hot gas can apparently be strongly affected by AGN activity- direct evidence of the ability of SMBHs to influence environment on large scales